

Combining metabolomics and network analysis to improve tacrolimus production in *Streptomyces tsukubaensis* using different exogenous feedings

Cheng Wang^{1,2} · Jiao Liu^{1,2} · Huanhuan Liu^{1,2} · Shaoxiong Liang^{1,2} · Jianping Wen^{1,2}

Received: 19 May 2017 / Accepted: 31 July 2017 / Published online: 3 August 2017
© Society for Industrial Microbiology and Biotechnology 2017

Abstract Tacrolimus is widely used as an immunosuppressant in the treatment of various autoimmune diseases. However, the low fermentation yield of tacrolimus has thus far restricted its industrial applications. To solve this problem, the time-series response mechanisms of the intracellular metabolism that were highly correlated with tacrolimus biosynthesis were investigated using different exogenous feeding strategies in *S. tsukubaensis*. The metabolomic datasets, which contained 93 metabolites, were subjected to weighted correlation network analysis (WGCNA), and eight distinct metabolic modules and seven hub metabolites were identified to be specifically associated with tacrolimus biosynthesis. The analysis of metabolites within each metabolic module suggested that the pentose phosphate pathway (PPP), shikimate and aspartate pathway might be the main limiting factors in the rapid synthesis phase of tacrolimus accumulation. Subsequently, all possible key-limiting steps in the above metabolic pathways were further screened using a genome-scale metabolic network model (GSMM) of *S. tsukubaensis*. Based on the prediction results, two newly identified targets (*aroC* and *dapA*) were overexpressed experimentally, and both of the engineered strains

showed higher tacrolimus production. Moreover, the best strain, HT-*aroC/dapA*, that was engineered to simultaneously enhanced chorismate and lysine biosynthesis was able to produce 128.19 mg/L tacrolimus, 1.64-fold higher than control (78.26 mg/L). These findings represent a valuable addition to our understanding of tacrolimus accumulation in *S. tsukubaensis*, and pave the way to further production improvements.

Keywords Tacrolimus · Exogenous feeding · Metabolomics · Metabolic network · *S. tsukubaensis*

Introduction

Tacrolimus (FK506), a 23-membered macrolide polyketide, is well known for its immunosuppressant activity and can be used to prevent graft rejection after allogeneic kidney, liver and heart transplantations [2, 3, 22, 46]. It has also been successfully applied in the treatment of inflammatory skin diseases, and is being investigated for therapeutic effects in other autoimmune diseases, including rheumatoid arthritis, ulcerative colitis, and Crohn's disease [1, 5, 23]. However, owing to the low titers obtained to date through microbiological synthesis, the cost of use of tacrolimus in the clinical therapy is very high. Ever since tacrolimus was first isolated from *Streptomyces tsukubaensis* no. 9993 by the Fujisawa Pharmaceutical Company in 1987, it has attracted increasing attention from a number of research groups, due to the aforementioned pharmaceutical potential and broad clinical applications [10, 24, 27, 34, 36, 37, 50, 61].

The biosynthesis of the tacrolimus macrolactone is mediated by the polyketide synthase (PKS)/non-ribosomal peptide synthetase (NRPS) system, comprising multiple-fatty acid synthase-like domains arranged in sets of modules [16].

Electronic supplementary material The online version of this article (doi:10.1007/s10295-017-1974-4) contains supplementary material, which is available to authorized users.

✉ Jianping Wen
jpwen@tju.edu.cn

¹ Key Laboratory of Systems Bioengineering (Ministry of Education), Tianjin University, Tianjin 300072, People's Republic of China

² SynBio Research Platform, Collaborative Innovation Center of Chemical Science and Engineering (Tianjin), School of Chemical Engineering and Technology, Tianjin University, Tianjin 300072, People's Republic of China

Specifically, the biosynthesis of tacrolimus begins with an unusual chorismate-derived unit (4R,5R)-4,5-dihydroxycyclohex-1-enecarboxylic acid (DHCHC) [3]. Subsequently, ten successive extender units (including two malonyl-CoA, five methylmalonyl-CoA, two methoxymalonyl-ACP and a unique allylmalonyl-CoA) are assembled into a polyketide chain by PKS [3, 15, 34]. The linear polyketide chain is subsequently condensed with lysine-derived piperolate by NRPS and the macrolide ring is formed by cyclization. Finally, the ring is further modified by two post-PKS processing reactions to form the final product (tacrolimus) [9]. Compared with the traditional strategies for tacrolimus overproduction (i.e., random mutagenesis, optimization of culture media and process conditions) [15, 26, 33, 51, 62], the identification of the entire tacrolimus biosynthesis genes cluster [17, 35] and the subsequent elucidation of the full genome sequence [4] enabled the development of more rational strategies for tacrolimus overproduction. For example, the exogenous feeding of tacrolimus precursors in the culture media has been regarded as an efficient and economical strategy to increase the yield. These precursors included methyl oleate [34], vinyl pentanoate [37], shikimate [21], picolinic acid, nicotinic acid and salicyl alcohol [49, 50], amino acids (i.e., lysine, proline, leucine, etc.) [21, 61], and so on. At the same time, the copy number increase of tacrolimus biosynthetic genes and the modification of the specific regulatory genes (*fkbN*, *fkbR*, *tcs2*, *tcs7* and *allN*) were also able to effectively improve tacrolimus production [8, 16, 37, 38, 40, 64]. Additionally, the genome-scale static/dynamic metabolic network model had been applied to search for the bottlenecks of tacrolimus biosynthesis [19, 52] and several potential genetic targets have been predicted that promise to enable an improved yield of tacrolimus.

Metabolomics has been widely applied as a powerful tool to describe the comprehensive metabolic status of a microorganism, as well as to reveal dynamic metabolic responses to exogenous or endogenous disturbances by analyzing the diversity and abundance of small-molecule metabolites [12, 13, 28, 57]. The most common statistical approaches used in metabolomics are principal component analysis (PCA) and partial least squares discriminant analysis (PLS-DA). PCA and PLS-DA are used not only to convert metabolomic data into a qualitative visual presentation (scores plot), but also to cluster biological samples into groupings based on similarity or difference [58]. Furthermore, a new approach named weighted correlation network analysis (WGCNA) has been recently proposed to describe the correlation relationships between clusters of highly correlated genes, proteins, metabolites or modules and external conditions or sample traits [42]. This approach can be used to reflect the continuous nature of the underlying co-expression information, and avoids information loss by setting artificial threshold parameters [42, 47, 48, 53, 55, 63]. With the help of appropriate

statistical and visualization tools, metabolomic analysis has recently been applied to identify key metabolites or pathways associated with various biochemical products in different *Streptomyces* species, including the intracellular metabolic responses to salt stress and nutrient depletion in *S. coelicolor* [28, 57], intracellular amino acid responses of *Streptomyces lydicus* to different pitching ratios [13], metabolomic profiling of *S. lydicus* E9 following the addition of glutamate and proline [12], and comparative metabolomic profiling of *S. hygroscopicus* and *S. tsukubaensis* to enhance rapamycin and tacrolimus production, respectively [61, 65]. These results demonstrated that metabolomics is a valuable tool for analyzing cell metabolism and the intracellular responses to environmental changes. However, even though several exogenous feeding strategies for improving tacrolimus overproduction have been reported, to our best knowledge, the dynamic response mechanisms of intracellular metabolism and the key-limiting steps of the corresponding pathways have not been systematically analyzed to date.

In this study, the intracellular metabolic responses to the enhancement of four synthetic precursor pathways in tacrolimus biosynthesis have been evaluated via the individual exogenous feeding of malonate, lysine, shikimate and citrate. Using metabolomic datasets obtained by gas chromatography-mass spectrometry (GC-MS) and liquid chromatography-mass spectrometry/mass spectrometry (LC-MS/MS), WGCNA was applied to reveal the metabolic response modules and hub metabolites highly associated with tacrolimus accumulation during the fermentation time course. These results indicated the pentose phosphate, shikimate and aspartate pathways showed higher positive correlations with tacrolimus production than other precursor pathways during the rapid synthesis phase. Combined with the GSMM model of *S. tsukubaensis*, we predicted several possible key-limiting steps in the identified metabolic pathways. The best strain (HT-*aroC/dapA*) produced 128.19 mg/L of tacrolimus, which was 1.64-fold higher than the result obtained with the parent strain under the same conditions.

Materials and methods

Strains, plasmids and culture conditions

The parent strain *S. tsukubaensis* D852, which was stocked in our laboratory and deposited in China General Microbiological Culture Collection Center with the accession number CGMCC 7180, was used in this work. *E. coli* JM109 was used to propagate all plasmids according to standard molecular biology procedures [44]. The integrative *E. coli*-*Streptomyces* vector pIB139 containing the *ermE** promoter (P_{ermE*}) was used for gene overexpression in *S. tsukubaensis* [59]. *E. coli* ET12567/pUZ8002

was used as the nonmethylating plasmid donor strain for intergeneric conjugation with *S. tsukubaensis* [25]. *E. coli* strains were cultured in Luria–Bertani (LB) medium at 37 °C. All strains and plasmids used in this work are listed in the supplementary material (Supplementary Materials A: Table S1).

The spores and seed culture of *S. tsukubaensis* were performed as the previously described methods of Xia et al. [61] and Martínez-Castro et al. [31], respectively. A total of 1 mL seed culture was transformed into 100 mL fermentation medium of a 500 mL Erlenmeyer flask and inoculated at 28 °C and 220 rpm for 7 days. The batch fermentation medium contained 20.0 g/L glucose, 40 g/L dextrin, 2.5 g/L soybean oil, 1 g/L NaCl, 2 g/L (NH₄)₂SO₄, 1 g/L K₂HPO₄, 2 g/L CaCO₃, 1 g/L MgSO₄·7H₂O, 0.001 g/L FeSO₄·7H₂O, 0.001 g/L MnCl₂·4H₂O, and 0.001 g/L ZnSO₄·7H₂O, and adjusted to pH 7.0 before autoclaving. Four kinds of metabolites (lysine, sodium citrate, sodium malonate, and sodium shikimate) were first prepared with sterilized water and filtered by 0.22 μm filter. Then, the sterile solutions of these metabolites were added into the medium with the final concentration 0.05 g/L after 30 h cultures, respectively.

Gene cloning, plasmid construction and transformation

All DNA manipulation and transformation of *Streptomyces* were prepared using the standard protocols [44]. The chorismate synthase (CHS) gene (*aroC*, STSU_29556) and dihydrodipicolinate synthase (DHDPS) gene (*dapA*, STSU_08193) were amplified from *S. tsukubaensis* genomic DNA by PCR amplification using the corresponding primer pairs (Supplementary Materials A: Table S2), respectively. Specifically, the gene *aroC* and *dapA* were digested by *NdeI*-*XbaI* and then inserted into the same site of pIB139 to obtain pAROC and pDAPA, respectively. For the plasmid construction of two genes co-overexpression, PCR product of *aroC* was digested with *NdeI*-*HindIII*, and cloned into the same sites of pUC18, generating pUC18-C. PCR product of *dapA* was digested with *HindIII*-*XbaI* and cloned into the *HindIII*-*XbaI* sites of pUC18-C, generating pUC18-CA. Then, pUC18-CA was digested with *NdeI*-*XbaI* and the long fragment containing the two genes was transferred to the same sites of pIB139, yielding pCA. After these plasmids were constructed, they would be transferred into *E. coli* ET12567/pUZ8002, and separately introduced into *S. tsukubaensis* through conjugal transfer [25]. Finally, the engineered strains of HT-*aroC* and HT-*dapA* would be obtained and the positive exconjugants were verified by PCR amplification and DNA sequencing with the corresponding primer pairs. The positive exconjugant of HT-*aroC/dapA* was verified by PCR amplification and DNA sequencing with primer pair pIB-F/pIB-R (Supplementary Materials A: Table S2).

Analytical methods

Dry cell weight was determined by washing twice with deionized water after centrifuging at 8000 rpm for 10 min, and then drying at 80 °C to constant weight. The residual total glucose in fermentation broth was quantified using phenol–sulfuric acid method [61]. Inorganic nitrogen (NH₄⁺-form) was quantified using the indophenol method [56, 60]. Inorganic phosphorus (PO₄³⁺-form) content was assayed with the ammonium molybdate spectrophotometric method [11, 60]. Tacrolimus was extracted and quantified by the previous described methods [21, 61].

Analysis of in vitro enzyme activities

The samples for enzyme activity measurement were harvested after 72 and 144 h cultures, respectively, and prepared as the reported methods [20]. The CHS activity was measured by monitoring the formation of chorismate at 275 nm as previously described [7]. The enzyme activity of DHDPS was determined as described by Laber et al. [29]. Total protein concentrations were quantified by Bradford assay with a reagent solution (Quick Start Bradford Dye, BioRad). The assays of enzyme activities were normalized to the total protein.

The identification of the key-limiting steps in the significant precursor pathways

Based on the constructed GSMM model of *S. tsukubaensis* by our group [19], the previous model had been further supplemented and completed, including filling of metabolic gaps, correcting of reaction directions and adding the exchange reactions (Supplementary Materials B). In this work, the identified metabolic pathways, which showed highly positive association with tacrolimus biosynthesis under different exogenous feeding treatments, would be selected to predict the possibly effective targets of enhancing tacrolimus production (Supplementary Materials A: Table S3). After the model was validated under the present cultural condition, the overexpressed targets would be predicted by the previous reported methods [19]. In brief, the intracellular metabolic fluxes could be firstly calculated by flux balance analysis (FBA) algorithm, and then the flux of the candidate reaction would be amplified to some extent (for instance 2.0-fold). Subsequently, a new set of intracellular metabolic fluxes would be calculated by minimization of metabolic adjustment (MOMA) algorithm. In the above process, MOMA employs quadratic programming to identify a point in flux space, which is closest to the initial flux, compatibly with the flux adjustment constraint [30].

The identification of targets was performed by comparing a fraction value, f_{PH} (the ratio of weighted and dimensionless

specific growth rate and specific tacrolimus production rate) [6, 19, 32]:

$$f_{\text{PH}} = f_{\text{Biomass}} \times f_{\text{FK506}} = (C_{\text{Biomass, model}}/C_{\text{Biomass, wild}}) \times (C_{\text{FK506, model}}/C_{\text{FK506, wild}})$$

The target with a higher f_{PH} value would be considered as the better candidate for improving tacrolimus production.

GC–MS and LC–MS/MS analysis

In order to analyze the intracellular metabolic response of *S. tsukubaensis* on different exogenous feedings, GC–MS and LC–MS/MS were performed for intracellular metabolites analysis. The cells collected at 6, 24, 48 and 72 h after feeding would be immediately quenched by 60% methanol (–40 °C, v/v) after taking from the fermentation broth. Then, the extraction, determination and analysis of intracellular metabolites were performed according to the previous described methods [61]. Succinic d₄ (St. Louis, MO, USA) and D-sorbitol-¹³C₆ (St. Louis, MO, USA) would be added in advance and served as the internal standard for GC–MS analysis and LC–MS/MS analysis, respectively. LC–MS/MS measurements of metabolites only included sugar phosphate intermediates of PPP and glycolysis, such as glucose 6-phosphate, fructose 6-phosphate, fructose 1,6-bisphosphate, glyceraldehyde 3-phosphate, phosphoenolpyruvate, erythrose 4-phosphate, ribose 5-phosphate, ribulose 5-phosphate, xylulose 5-phosphate and sedoheptulose 7-phosphate. All the chemicals used in the metabolome isolation, GC–MS and LC–MS/MS analysis were purchased from Sigma-Aldrich.

WGCNA network construction

A metabolic correlation network was established from the GC–MS and LC–MS/MS data sets by calculating weighted Pearson correlation matrices relative to metabolites abundance firstly. And the standard procedure of WGCNA would be performed to create the networks through the previous reports [42, 53]. Briefly, connection strength matrices would be first created from the transformation of weighted correlation matrices by a power function, and then used to calculate topological overlap (TO). The metabolites with highly similar correlation relationships would be grouped into the same modules through hierarchical clustering based on the results of TO. Subsequently, average linkage hierarchical clustering was performed to obtain metabolite dendrograms. The module assignment determined by the Dynamic Tree Cut of WGCNA was distinguished with the color row underneath the dendrograms. The modules with correlation $r \geq 0.5$ and statistical significance p value less than 0.05 were extracted for further investigation. Hubs metabolites were screened by high connectivity with other metabolites (>5) in the distinct

modules by exporting the WGCNA network to VisANT and Cytoscape for network visualization [42].

Data processing and multivariate statistical analysis

The peak area of each metabolite was normalized to the internal standard succinic acid d₄ and cell biomass in GC–MS analysis. Absolute metabolite concentrations determined by LC–MS/MS in extracts were normalized to the biomass and internal standard D-sorbitol-¹³C₆. Both of the normalized metabolites between GC–MS and LC–MS/MS analysis were combined together finally. The relative abundance matrix of the whole identified metabolites at each sampling time point was imported into SIMCA-P package (Ver 11.5; Umetrics, Umea, Sweden) for the multivariate statistical analysis. In this study, five biological replicates were used to perform multivariate analysis for each sample condition, and the experimental data were calculated as the mean value with the error indicated by the standard deviation.

Results

Fermentation properties under different exogenous feedings

The main goal of the various exogenous feeding strategies tested in this study was to enhance precursor synthesis for tacrolimus overproduction, building upon earlier work [3]. It would be more effective and intuitive to understand the dynamic responses of intracellular metabolism by directly disturbing the carbon fluxes of the precursor pathways of tacrolimus biosynthesis and examining the consequences. On the basis of literature research, the exogenous feeding of shikimate, malonate, lysine and citrate were very effective on tacrolimus overproduction by directly enhancing the fluxes in the shikimate pathway, malonyl-CoA synthesis, lysine metabolism and TCA cycle, respectively [3, 15, 54, 61]. Therefore, considering the simple structure and availability of these precursors, all four was finally selected for the exogenous feeding experiments.

Aiming at finding the features of different exogenous feeding strategies, the key fermentation parameters were first compared with the basic culture medium. As shown in Fig. 1, while a similar fermentation tendency was found among all feeding treatments, obvious difference could also be observed in pH values, substrates consumption (total glucose, NH₄⁺ and PO₄³⁺), biomass and tacrolimus accumulation. For example, all of the cultures undergoing exogenous feedings displayed higher substrate consumption rates than

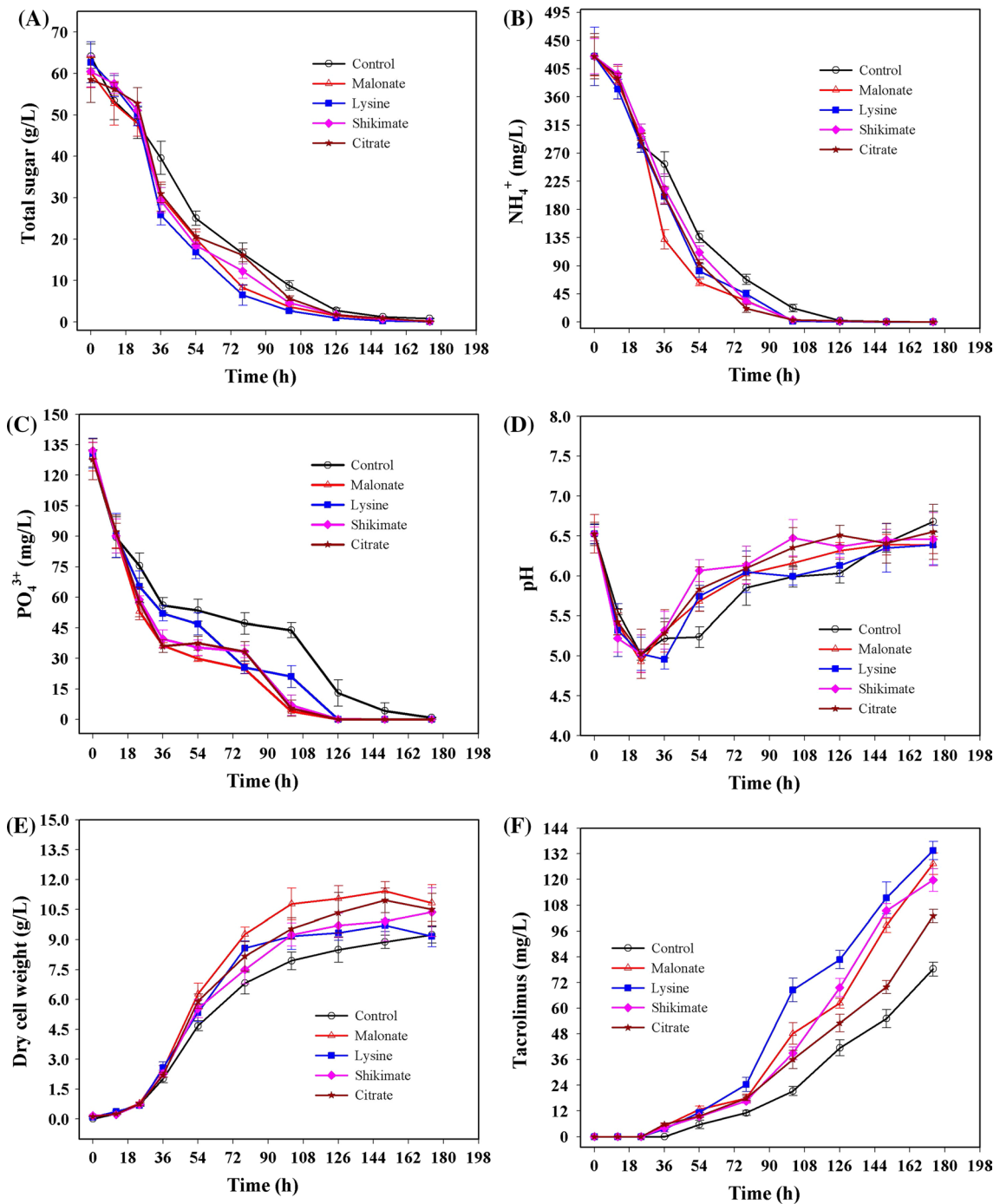


Fig. 1 The fermentation properties of *S. tsukubaensis* under different exogenous feeding (malonate, lysine, shikimate and citrate). **a** total glucose, **b** inorganic ammonium (NH_4^+ -form), **c** inorganic phosphorus (PO_4^{3+} -form), **d** pH, **e** dry cell weight, **f** tacrolimus concentration

the control (Fig. 1a-c). Cell growth was enhanced significantly by all exogenous feeding treatments compared with the control (Fig. 1e). Furthermore, an earlier starting point of tacrolimus biosynthesis than in the control, at 6 h after commencing exogenous feeding, was found in all treatments (Fig. 1f). The final tacrolimus concentrations in the lysine, malonate, shikimate and citrate feeding strains had

reached to 133.49 ± 4.25 , 127.32 ± 5.02 , 119.73 ± 5.26 and 103.01 ± 3.05 mg/L, respectively, significantly higher than the control (78.26 ± 3.26 mg/L). Moreover, the strains fed with malonate, shikimate and citrate showed higher final biomass concentrations than the control (9.24 ± 0.41 g/L), such as 10.83 ± 0.91 , 10.37 ± 1.22 and 10.5 ± 0.8 g/L for malonate, shikimate and citrate, respectively. Interestingly,

the lysine feeding strain had a higher biomass concentration during the exponential and early-stable phases, while its final biomass yield (9.17 ± 0.52 g/L) was lower than that of the control. These results suggested that the intracellular metabolism was perturbed obviously and that additional carbon flux was rerouted towards tacrolimus biosynthesis under the exogenous feeding treatments.

Differential effects of precursor feedings on metabolomic profiles

In the previous study, we developed an optimized protocol for GC–MS and LC–MS/MS analysis, which enabled to identify more than 98 metabolites from *S. tsukubaensis*, encompassing sugars, amino acids, organic acids, fatty acids and so on [61]. Using the same analytical method, a total of 93 intracellular metabolites, including 83 metabolites by GC–MS analysis and 10 sugar phosphate by LC–MS/MS analysis (Supplementary Materials A: Table S4), were identified in 100 samples at the different sampling times (i.e., 6, 24, 48 and 72 h after exogenous feeding) for all treatment conditions. PCA score plots of the corresponding metabolomic profiles were compared between the control and all exogenous feeding treatments (Fig. 2).

Analysis of the score plots revealed the following features: (1) all of the same treated samples at different time points could be obviously clustered together, respectively,

and separated with other time point samples completely; (2) the differently treated samples collected at the same time point could also be clustered together clearly; (3) a clear change trend of the metabolomic profiles across the time courses could be found among all exogenous feeding strategies. Interestingly, a remarkable regularity of intracellular metabolism could also be clearly observed along the time course. For example, the differences of metabolomic profiles in different feeding treatments were gradually reduced from 6 to 48 h (in the exponential phase), but an increasing difference reappeared at the stationary phase (at 72 h after feeding). A possible reason may be that cell growth played a dominant role in the exponential phase, while some metabolic differences still existed in all of the samples. Meanwhile, the metabolic differences resulting from the different feeding treatments may not have disappeared, and still remained in a “masked” state beneath the heavy growth-related fluxes until the stationary phase. Although the molecular details are still unknown, the different effects of exogenous feeding strategies merit further investigation.

WGCNA correlation network construction

In order to analyze the intracellular metabolic responses to tacrolimus synthesis among all the exogenous feeding treatments, a WGCNA was constructed to identify the significant metabolic modules and hub metabolites highly associated

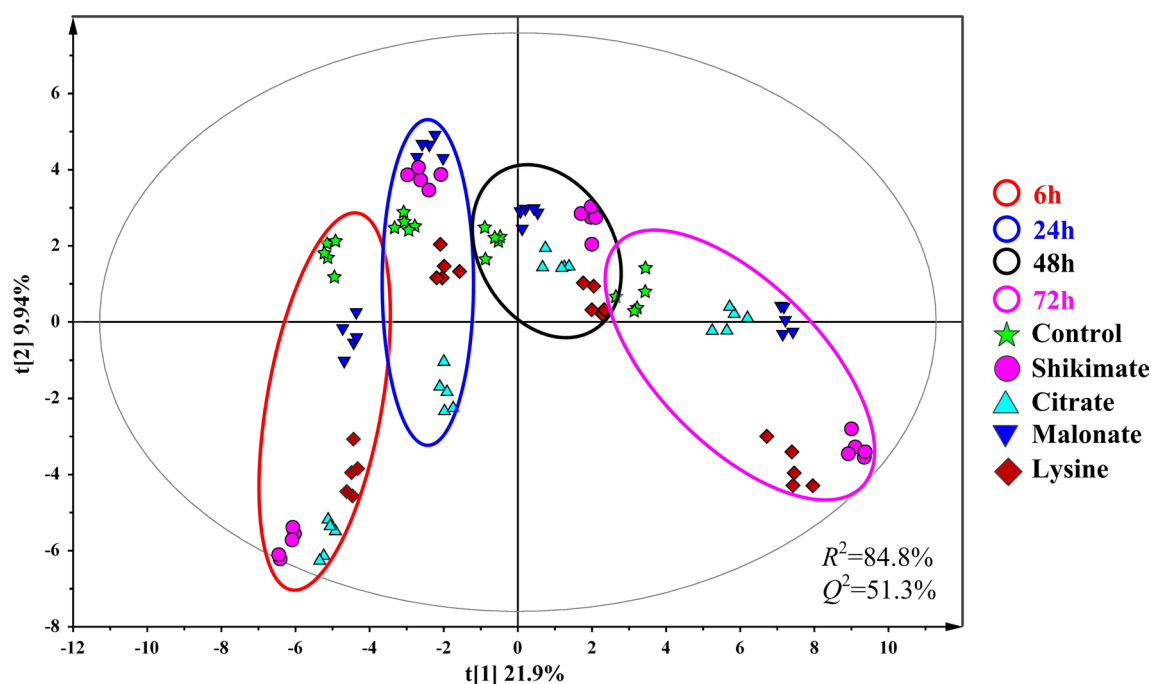


Fig. 2 PCA analysis of GC–MS and LC–MS/MS metabolomic profiles. Score plot of fermentation samples collected at 6, 24, 48, and 72 h after feeding, respectively. The culture medium was supple-

mented with 0.05 g/L shikimate, citrate, malonate and lysine after 30-h cultivation, respectively

with tacrolimus biosynthesis across the time courses. Using the GC–MS and LC–MS/MS datasets, 4 (M6h-F1, M6h-F2, M6h-F3 and M6h-F4), 1 (M24h-F1), 1 (M48h-F1) and 2 (M72h-F1 and M72h-F2) distinct metabolic modules were identified successfully at 6, 24, 48 and 72 h after exogenous feedings, respectively (Table 1; Fig. 3).

The metabolites within the modules from different time points showed great differences. For example, the most modules could be found at 6 h after feeding, and several metabolites in these modules (M6h-F1, M6h-F2, M6h-F3 and M6h-F4) were involved in central carbohydrate metabolism and amino acid metabolism. Furthermore, the enhancement of several precursor pathways in tacrolimus biosynthesis was also observed based on their respective specific metabolites, such as pipercolate, malonic acid, shikimate, phosphoenolpyruvate and erythrose 4-phosphate. Compared with the control, an earlier start-point of tacrolimus synthesis was also found in the all feeding treatments (Fig. 1f). Among all the sampling time points, M24h-F1 and M48h-F1 were identified in the exponential phase (at 24 and 48 h after feeding, respectively). A possible reason is that the rapid growth of bacteria might take precedent over all other cellular processes in the exponential phase, including over tacrolimus biosynthesis. In agreement with this idea, sugar phosphate intermediates and organic acid were found in the module M24h-F1 and M48h-F1 (Table 1). During the stationary phase (at 72 h after feeding), analysis of the metabolites within each module (M72h-F1 and M72h-F2) indicated that a part of the precursor synthesis pathways showed a high correlation with tacrolimus production. These

included the shikimate pathway (i.e., phosphoenolpyruvate, tryptophan and phenylalanine) and aspartate pathway (i.e., aspartic acid, isoleucine, methionine and threonine). At the main phase of tacrolimus accumulation, the enhancement of shikimate and aspartate pathways would provide additional amounts of important precursors, such as DHCHC, pipercolate and propionyl-CoA.

Hub metabolites possess a high degree of connectivity in biological interaction networks and consequently have high biological importance [63]. In accordance with the results, only the modules in the rapid synthesis phase of tacrolimus production (M48h-F1, M72h-F1 and M72h-F2) were used to further analysis of hub metabolites. A total of 3 (pyruvate, phosphoenolpyruvate and methylmalonate) and 4 (leucine, methionine, tryptophan and phenylalanine) hub metabolites were significantly associated with the modules of 48 and 72 h, respectively (Fig. 4). In the M48h-F1 module, the hub metabolites of pyruvate, phosphoenolpyruvate and methylmalonate were located in the key nodes for DHCHC and methylmalonyl-CoA synthesis, all of which are necessary tacrolimus precursors [3]. Among the hub metabolites in the modules M72h-F1 and M72h-F2, three metabolites (leucine, tryptophan and phenylalanine) had been confirmed to promote tacrolimus production by exogenous feeding [61]. Methionine was first found to show a high connectivity with other metabolites and to have a strong correlation with tacrolimus synthesis. In fact, methionine could transform into acetyl-CoA or propionyl-CoA via its degradation pathway [14], both of which are the important coenzyme A sources in tacrolimus biosynthesis. These identified hub metabolites

Table 1 Member metabolites clustered into each of tacrolimus-responsive modules

Module	Association	<i>p</i> value	Metabolites
M6h-F1	<i>r</i> = 0.56	<i>p</i> = 0.004	Fructose 6-phosphate, fructose 1,6-bisphosphate, 6-phospho-D-gluconate, glyceraldehyde 3-phosphate, glycerate 3-phosphate, sedoheptulose 7-phosphate, glucose 6-phosphate, homocystine, erythrose 4-phosphate, glucose, homoserine, oxaloacetate, docosanoic acid, malonic acid, maltose
M6h-F2	<i>r</i> = 0.54	<i>p</i> = 0.006	Adenosine, trehalose, ribulose 5-phosphate, uracil, thymidine, xylulose 5-phosphate, leucine, nonanedioic acid, glycerol 3-phosphate, linoleic acid, citrate, decanedioic acid
M6h-F3	<i>r</i> = 0.71	<i>p</i> = 6e–05	Norleucine, glycine, serine, methionine, 1,3-butanediol, succinate, fumarate, 2-oxoglutarate, guanine, malate, pipercolate, allothreonine, benzoic acid, threonine, ornithine, 2-oxobutanoate, acetone
M6h-F4	<i>r</i> = 0.73	<i>p</i> = 3e–05	Pyruvate, ribose 5-phosphate, indole, isoleucine, glycerol, phosphoenolpyruvate, pentanoic acid, valine, glucitol, n-pentadecanoic acid, hexadecanoic acid, butanal, tryptophan, tryptophol, shikimate
M24h-F1	<i>r</i> = 0.89	<i>p</i> = 3e–09	Fructose 6-phosphate, decanedioic acid, fructose 1,6-bisphosphate, glucose 6-phosphate, glycerol, homocystine, glyoxylic acid, cadaverine, trehalose, acetoin, ethanedioic acid, norleucine, glucuronic acid, glucose
M48h-F1	<i>r</i> = 0.75	<i>p</i> = 2e–05	Nonanoic acid, valine, ethanol, erythrose 4-phosphate, malonic acid, nicotinate, rhamnose, acetone, methylmalonate, ribulose 5-phosphate, glycerol 3-phosphate, sedoheptulose 7-phosphate, pyruvate, xylulose 5-phosphate, indole, heptadecanoic acid, glycine, allothreonine, phosphoenolpyruvate, proline, benzoic acid, urea, acetoin
M72h-F1	<i>r</i> = 0.77	<i>p</i> = 8e–06	Isoleucine, uracil, norleucine, methionine, ribose 5-phosphate, glycine, valine, leucine, cadaverine
M72h-F2	<i>r</i> = 0.53	<i>p</i> = 0.006	Docosanoic acid, aspartic acid, 2-oxobutanoate, glutamic acid, pentanoic acid, niacinamide, phosphoenolpyruvate, octadecanoic acid, ornithine, galactose, threonine, tryptophan, phenylalanine, pyruvate, oleic acid

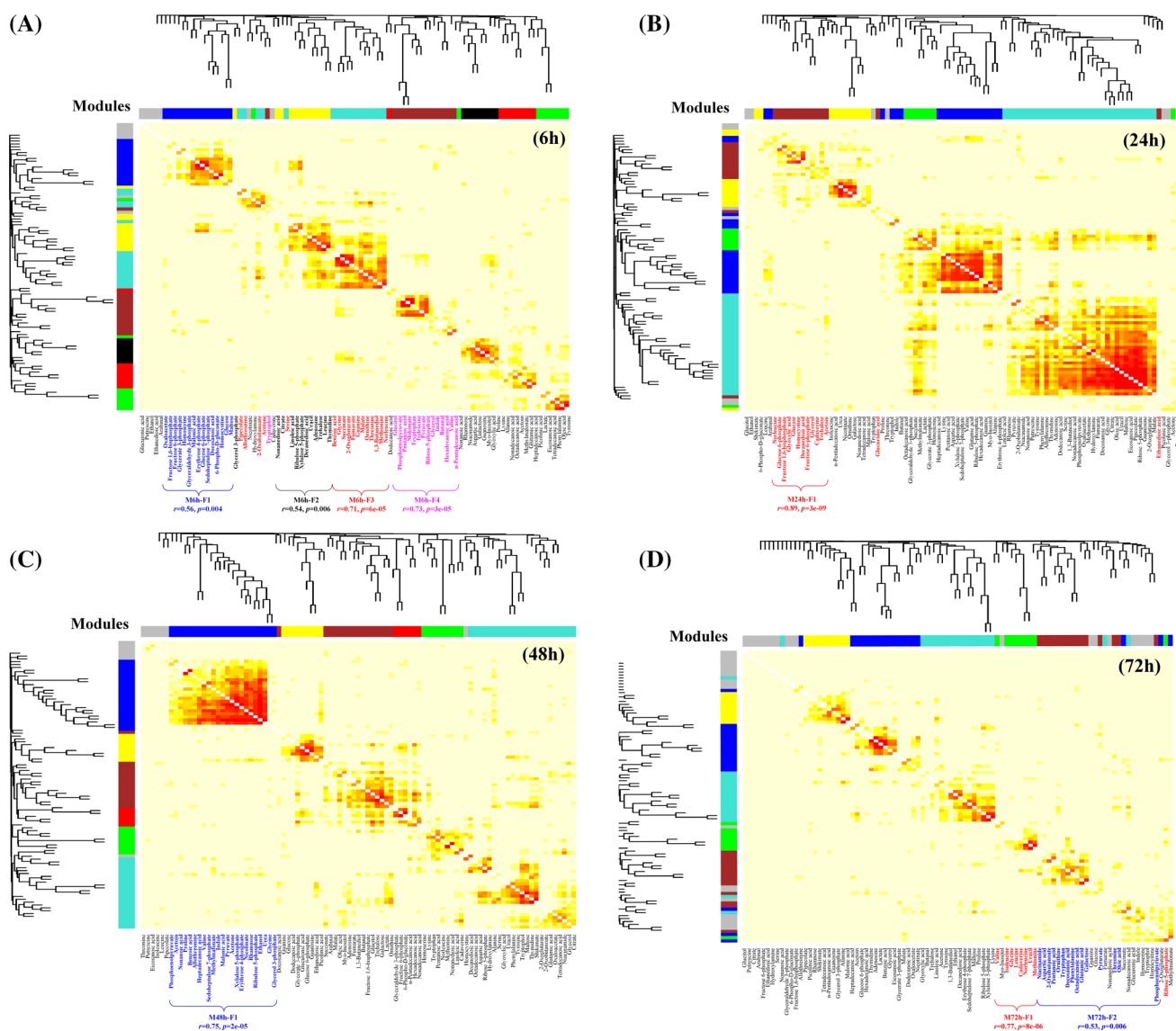


Fig. 3 WGCNA of metabolic profiles of *S. tsukubaensis* highly associated with tacrolimus biosynthesis under different exogenous feedings. Fermentation samples were collected at 6 h (a), 24 h (b), 48 h (c), and 72 h (d) after exogenous feeding, respectively. The heatmap depicts the topological overlap (TO) matrix among 93 metabolites in the analysis. Light color represents low TO and progressively darker red color represents higher TO. Blocks of darker colors along the

diagonal are the modules. The metabolites dendrogram and module assignment are also showed along the left side and the top. The modules highly associated with tacrolimus production ($r \geq 0.5$ and p value < 0.05) are indicated with their metabolites within the modules in different colors, and the correlation coefficients and p values are listed below the modules (color figure online)

might not only serve as biomarkers for tacrolimus synthesis, but also specifically indicate that the shikimate and aspartate pathways might be very important for tacrolimus synthesis during the stationary phase.

Prediction of potential targets based on in silico simulations

In a quasi-steady state metabolic model, there are an infinite number of flux distributions that satisfy the GSMM model

so that the subspace of allowed flux distributions needs to be further constrained by boundary conditions to obtain an optimal flux distribution [18]. In this work, total glucose (including dextrin, which can be hydrolyzed by the cells to yield glucose [43]), inorganic nitrogen (NH_4^+ -form), inorganic phosphorus (PO_4^{3+} -form) and tacrolimus production were calculated as the model constraints based on the existing culture conditions. For instance, the specific uptake rates of glucose, NH_4^+ and PO_4^{3+} were set to 1.259, 0.0913 and 0.0476 mmol/g DCW/h, respectively. At the same time, the

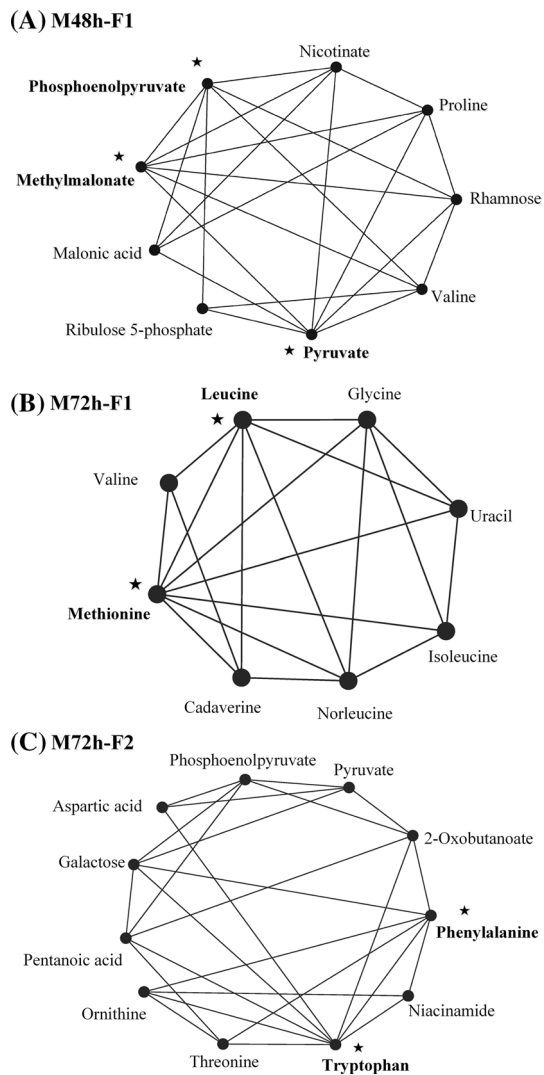


Fig. 4 Hub metabolites and their metabolic profiles as represented by node and edge graph. **a** Pyruvate, phosphoenolpyruvate and methylmalonate for M48h-F1; **b** leucine and methionine for M72h-F1; **c** tryptophan and phenylalanine for M72h-F2

experimental specific production rate of tacrolimus was determined to be $0.1069 \mu\text{mol/g DCW/h}$ and was set as the lower bound for the tacrolimus exchange reaction. Using the experimentally determined values, the specific growth rate of GSMM was predicted to be 0.037 h^{-1} , which was basically consistent with the experimental data (0.042 h^{-1}).

According to the analysis of these distinct modules, several metabolites derived from PPP, shikimate and aspartate pathways had been identified as having highly positive correlations with tacrolimus production during its rapid synthesis phase (Table 1). However, the key-limiting steps of these metabolic pathways could not be identified accurately. Thus, to find the key-limiting steps, the above three metabolic pathways were screened to predict the effective overexpression targets using the GSMM model. As shown in Fig. 5, all

of the potential targets were identified and ranked by their f_{PH} values. Among all predicted overexpression targets, the most effective targets were found in PPP. These included r56 (Glucose-6-phosphate 1-dehydrogenase, $f_{\text{PH}} = 30.95$), r57 (6-phosphogluconolactonase, $f_{\text{PH}} = 30.95$), r58 (Phosphogluconate dehydrogenase, $f_{\text{PH}} = 5.96$), r70 (Phosphoricmonoester hydrolases, $f_{\text{PH}} = 2.28$), r62 (Phosphoglucosmutase, $f_{\text{PH}} = 2.11$) and r64 (Transaldolase, $f_{\text{PH}} = 1.45$). The enhancement of flux in PPP could not only provide more reducing power (NADPH), but may also result in an increased flux of carbon to erythrose-4-phosphate, (a direct precursor of shikimate pathway), both of which are very important for improving tacrolimus production. In previous reports, several targets in PPP, such as glucose-6-phosphate dehydrogenase (r56) [19] and transketolase [52], were shown to play an effective role in improving tacrolimus titer. The next group of targets (r145, 2-dehydro-3-deoxyphosphoheptonate aldolase; r146, 3-dehydroquininate synthase; r149, Shikimate kinase; r151, Chorismate synthase) that were located in the shikimate pathway, had the same f_{PH} values ($f_{\text{PH}} = 14.86$). Overexpressing these targets may improve the pool of DHCHC, which is the starting unit of tacrolimus biosynthesis, by enhancing the shikimate pathway [3, 19]. Meanwhile, previous reports had also confirmed that overexpression of 3-deoxy-D-arabinoheptulosonate-7-phosphate synthase (r145) enhanced tacrolimus production by approximately 50% in *S. tsukubaensis* D852 [19]. Among the predicted targets in the aspartate branch, those targets in lysine biosynthesis pathway (i.e., r96, dihydrodipicolinate synthase; r97, Dihydrodipicolinate reductase; r98, 2,3,4,5-tetrahydropyridine-2-carboxylate N-succinyltransferase; r99, Succinyl-diaminopimelate aminotransferase; r100, Succinyl-diaminopimelate desuccinylase; r101, Diaminopimelate epimerase) had higher f_{PH} values ($f_{\text{PH}} = 3.36$), which would result in an increase of intracellular lysine flux and precursor pool (pipecolate), thus improving the product titer. Similar with lysine biosynthesis, the targets r93 (Aspartate kinase, $f_{\text{PH}} = 2.39$) and r94 (Aspartate-semialdehyde dehydrogenase, $f_{\text{PH}} = 2.39$) in the homoserine biosynthesis branch showed positive effects on tacrolimus overproduction, both of which were also beneficial for directly and indirectly improving the levels of lysine and pipecolate.

Effect of the targets overexpression manipulation on tacrolimus biosynthesis

According to the f_{PH} values, the three targets r56, r57 and r58 are all located in the initial step of the pentose phosphate pathway, which directly control the carbon flux into this pathway. Since a previous report had confirmed that overexpressing the target r56 was effective for tacrolimus overproduction [19], these three targets were excluded from the subsequent genetic manipulation study. Similarly, the

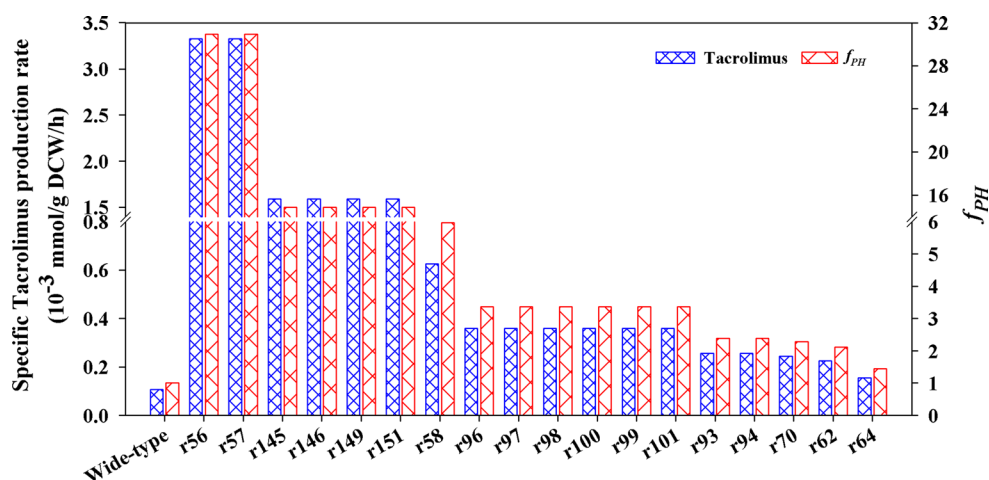


Fig. 5 The predicted results of the key-limiting targets by GSMM model in *S. tsukubaensis*. All of the candidate targets were selected from PPP, shikimate and aspartate pathways based on the WGCNA analysis. The detailed information of the all predicted targets was as following: *r56* glucose-6-phosphate 1-dehydrogenase, *r57* 6-phosphogluconolactonase, *r58* Phosphogluconate dehydrogenase, *r62* Phosphoglucomutase, *r64* Transaldolase, *r70* Phosphoric-monoester hydrolases, *r93* Aspartate kinase, *r94* Aspartate-semialdehyde dehy-

drogenase, *r96* dihydrodipicolinate synthase, *r97* Dihydrodipicolinate reductase, *r98* 2,3,4,5-tetrahydropyridine-2-carboxylate N-succinyltransferase, *r99* Succinyl-diaminopimelate aminotransferase, *r100* Succinyl-diaminopimelate desuccinylase, *r101* Diaminopimelate epimerase, *r145* 2-dehydro-3-deoxyphosphoheptonate aldolase, *r146* 3-dehydroquininate synthase, *r149* Shikimate kinase, *r151* chorismate synthase

target reactions *r145* and *r146* were not been considered as gene modification targets because the target *r145* had also been verified before [19]. By contrast, the target *r151* catalyzes the chorismate synthesis reaction, and thus may be capable of more directly increasing the chorismate concentration if overexpressed. Therefore, only *r151* was selected as a candidate for overexpression, while all four targets in the shikimate pathway had the same f_{PH} value. Among the predicted targets from lysine pathway, the target *r96* had been reported to catalyze the limiting step for lysine overproduction [41]. In fact, lysine metabolism was the only source of pipecolate in tacrolimus biosynthesis. Therefore, the increasing of lysine concentration would be benefit for improve tacrolimus yield. The gene corresponding to *r96* was, therefore, also considered for overexpression, while the rest of the predicted targets (*r97*, *r98*, *r100*, *r99* and *r101*) had the same f_{PH} values as *r96*. Finally, the targets from the shikimate pathway (*r151*) and lysine biosynthesis (*r96*) were selected for further experimental verification. To our delight, the final tacrolimus production was improved effectively in all the overexpression strains (Fig. 6). Moreover, the results of enzyme activity assays also further confirmed that the corresponding targets were successfully enhanced both in the exponential and the stationary phase (Table 2). Additionally, the different promoting effects of the selected targets on tacrolimus accumulation could also be observed clearly.

As is shown in Fig. 6, the engineered strain HT-*aroC* showed high tacrolimus production of up to 109.87 ± 8.26 mg/L, due to its enhanced shikimate pathway.

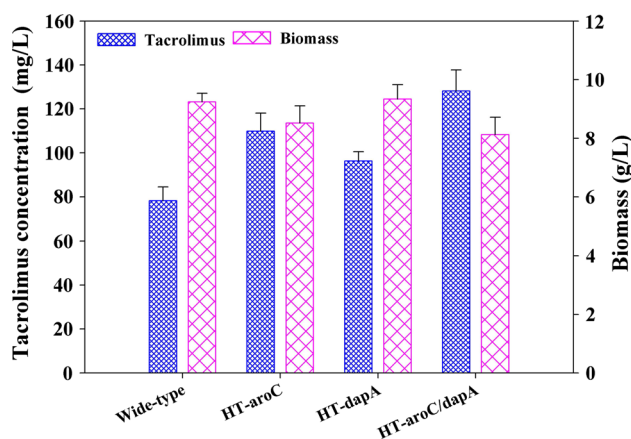


Fig. 6 The effect of genes overexpression manipulation on tacrolimus production and cell growth

Interestingly, a slight decrease of the final biomass concentration could be observed in the HT-*aroC* mutant. The DHDPS activity of the strain HT-*dapA*, which overexpresses the lysine synthesis gene *dapA*, was clearly increased both at 72 and at 144 h (Table 2). There was no significant change of cell growth (9.24 ± 0.29 g/L) in the engineered mutant, but tacrolimus production was nevertheless enhanced by approximately 23.14% (96.37 ± 4.19 mg/L), compared with the parent strain (78.26 ± 6.22 mg/L) (Fig. 6). According to the metabolomics analysis, a combined synergistic effect of enhancing chorismate and lysine biosynthesis

Table 2 Specific activity of enzymes by parent strain *S. tsukubaensis* and recombinants in batch cultures

Enzyme activity (U/ mg protein)	Time/h	Control	HT- <i>aroC</i>	HT- <i>dapA</i>	HT- <i>aroC/dapA</i>
CHS	72	0.05 ± 0.01	0.14 ± 0.01	–	0.12 ± 0.01
	144	0.02 ± 0.00	0.08 ± 0.00	–	0.07 ± 0.02
DHDPS	72	11.73 ± 1.23	–	29.26 ± 3.09	31.74 ± 2.30
	144	6.82 ± 0.86	–	14.53 ± 2.71	12.08 ± 1.58

simultaneously had also been performed by multiple genes overexpression manipulation (*aroC* and *dapA* together). The CHS and DHDPS activities of HT-*aroC/dapA* were indeed increased compared with the control, reaching, respectively, 3.5- and 1.77-fold higher values at 144 h (Table 2). Moreover, the HT-*aroC/dapA* mutant was able to produce 128.19 ± 9.57 mg/L tacrolimus, a 1.64-fold increase over the parent strain. Nevertheless, the growth of the HT-*aroC/dapA* strain was somewhat affected, leading to a lower final biomass concentration (8.12 ± 0.60 g/L) compared with the parent strain (9.24 ± 0.29 g/L).

Discussion

The higher-value immunosuppressant tacrolimus has exhibited a good therapeutic potential in the clinical treatment of a number of diseases. Owing to the complexity of its biosynthesis, several primary metabolic pathways have significant effects on its production. Therefore, considerable efforts have been made to improve tacrolimus production by various exogenous feeding strategies. However, the response mechanisms of intracellular metabolism under different exogenous feeding strategies has to our best knowledge not been reported before. Furthermore, the key-limiting steps among the many precursor pathways of tacrolimus synthesis still remained unknown, which further limited tacrolimus overproduction.

Metabolomics is considered to be more closely connected to the physiology of organisms than the other “omics” approaches (i.e., transcriptomics and proteomics) because the rate of enzymatic reactions is regulated directly by the concentrations of substrates and products in cells [39, 45]. We, therefore, selected four different exogenous feeding strategies targeting different precursor pathways to decipher the intracellular dynamic metabolic responses during tacrolimus production. Coupled with tacrolimus synthesis, WGCNA analysis identified several distinct metabolic modules and hub metabolites that were tightly associated with tacrolimus synthesis in different culture stages. Starting especially from the post-exponential phase (at 48 h after feeding), tacrolimus accumulated rapidly, so that several precursor synthesis pathways (i.e., methylmalonyl-CoA pathway, PPP pathway and shikimate pathway) quickly

started to become responsive to tacrolimus accumulation. Hub metabolites form the module M48h-F1 implied that pyruvate, phosphoenolpyruvate and methylmalonate had a high degree of connectivity during this phase. The metabolic flux node between pyruvate and phosphoenolpyruvate played important role in this key branch of tacrolimus precursors. For example, phosphoenolpyruvate is the starting point of DHCHC synthesis [3], and methylmalonate was the direct precursor of methylmalonyl-CoA [3]. Pyruvate can not only be transformed into methylmalonyl-CoA, but can also control the synthesis of acetyl-CoA in the central carbon metabolism, which in turn is an important node for the synthesis of the important tacrolimus precursor allylmalonyl-CoA [19]. Thus, balancing the flux of this key node would be very important during the rapid phase of tacrolimus synthesis. The analysis of the distinct metabolic modules and hub metabolites at 72 h indicated that the shikimate and aspartate pathways might directly control the final tacrolimus production. In fact, DHCHC, which is the starter unit for tacrolimus synthesis, is derived from shikimate pathway [3]. Isoleucine, methionine and lysine (aspartate pathway) can also be transformed into several necessary precursors, such as pipecolate and propionyl-CoA. Therefore, simultaneously enhancing these two metabolic pathways might further improve tacrolimus production during the stationary phase.

In addition to identifying the crucial metabolic pathways, another major goal of this study was to decipher the possible key-limiting steps in said pathways, and further improve tacrolimus production. Therefore, the GSMM model was applied to predict potential targets in PPP, shikimate and aspartate pathways. Several uncovered targets showed highly positive effects on tacrolimus production (Fig. 5). Following further experimental verification, the final tacrolimus production was improved markedly in all the resulting overexpression strains. Specifically, overexpressing the *aroC* gene from the shikimate pathway resulted in a higher tacrolimus yield, which indicated that this might be a key-limiting step in tacrolimus biosynthesis. In the lysine synthesis pathway, overexpressing the gene *dapA* also enhanced tacrolimus production effectively (up to 96.37 ± 4.19 mg/L). Additionally, simultaneously enhancing the flux in the shikimate and lysine pathways (HT-*aroC/dapA*) resulted in the highest tacrolimus yield (128.19 ± 9.57 mg/L) of all the engineered

strains, which was consistent with the metabolomic analysis. These results also showed that the strategy used in this work was effective for tacrolimus overproduction. Nevertheless, other detailed information of intracellular metabolism are still needed to improve and perfect the GSMM of *S. tsukubaensis* in the further, including metabolic regulation, ^{13}C metabolic analysis, thermodynamic and kinetic information. The addition of these information will be very important for further improving simulation accuracy, and by extension tacrolimus production in the further.

In conclusion, the GC–MS- and LC–MS/MS-based metabolomic analysis and a WGCNA network analysis of *S. tsukubaensis* under shikimate, citrate, malonate and lysine feeding regimens clearly showed that intracellular responses in the tacrolimus biosynthesis pathway were different, as evidenced by the strengthening of different precursor synthesis pathways under said regimens. Further, the PPP, shikimate and aspartate pathways were found to play crucial roles in tacrolimus biosynthesis. Based on the GSMM predictions, several potential targets were identified as the key-limiting steps in these metabolic pathways. Overexpression of some of the target genes further corroborated these predictions, and the final tacrolimus production in the resulting engineered strain HT-*aroC/dapA* was improved approximately 1.64-fold compared with the control. These findings, thus, lay the foundation for further improvements of tacrolimus production in the future.

Acknowledgements This work was financially supported by the National Natural Science Foundation of China (No. 21376171), the key technologies R & D program of Tianjin (No. 16YFZCSY00780), the National 973 Project of China (No. 2013CB733600), the Key Program of National Natural Science Foundation of China (No. 21236005).

References

- Akimoto K, Kusunoki Y, Nishio S, Takagi K, Kawai S (2008) Safety profile of tacrolimus in patients with rheumatoid arthritis. *Clin Rheumatol* 27:1393–1397
- Allison AC (2000) Immunosuppressive drugs: the first 50 years and a glance forward. *Immunopharmacology* 47:63–83
- Barreiro C, Martínez-Castro M (2014) Trends in the biosynthesis and production of the immunosuppressant tacrolimus (FK506). *Appl Microbiol Biotechnol* 98:497–507
- Barreiro C, Prieto C, Sola-Landa A, Solera E, Martínez-Castro M, Pérez-Redondo R, García-Estrada C, Aparicio JF, Fernández-Martínez LT, Santos-Aberturas J (2012) Draft genome of *Streptomyces tsukubaensis* NRRL 18488, the producer of the clinically important immunosuppressant tacrolimus (FK506). *J Bacteriol* 194:3756–3757
- Benson A, Barrett T, Sparberg M, Buchman AL (2008) Efficacy and safety of tacrolimus in refractory ulcerative colitis and Crohn's disease: a single-center experience. *Inflamm Bowel Dis* 14:7–12
- Boghigian BA, Lee K, Pfeifer BA (2010) Computational analysis of phenotypic space in heterologous polyketide biosynthesis—applications to *Escherichia coli*, *Bacillus subtilis*, and *Saccharomyces cerevisiae*. *J Theor Biol* 262:197–207
- Bornemann S, Lowe DJ, Thorneley RN (1996) The transient kinetics of *Escherichia coli* chorismate synthase: substrate consumption, product formation, phosphate dissociation, and characterization of a flavin intermediate. *Biochemistry* 35:9907–9916
- Chemler JA, Fowler ZL, McHugh KP, Koffas MA (2010) Improving NADPH availability for natural product biosynthesis in *Escherichia coli* by metabolic engineering. *Metab Eng* 12:96–104
- Chen D, Zhang L, Pang B, Chen J, Xu Z, Abe I, Liu W (2013) FK506 maturation involves a cytochrome p450 protein-catalyzed four-electron C-9 oxidation in parallel with a C-31 O-methylation. *J Bacteriol* 195:1931–1939
- Chen D, Zhang Q, Zhang Q, Cen P, Xu Z, Liu W (2012) Improvement of FK506 production in *Streptomyces tsukubaensis* by genetic enhancement of the supply of unusual polyketide extender units via utilization of two distinct site-specific recombination systems. *Appl Environ Microbiol* 78:5093–5103
- Chen P Jr, Tt Toribara, Warner H (1956) Microdetermination of phosphorus. *Anal Chem* 28:1756–1758
- Cheng J-S, Cui S-F, Ding M-Z, Yuan Y-J (2013) Insights into the roles of exogenous glutamate and proline in improving streptolydigin production of *Streptomyces lydicus* with metabolomic analysis. *J Ind Microbiol Biotechnol* 40:1303–1314
- Cheng J-S, Liang Y-Q, Ding M-Z, Cui S-F, Lv X-M, Yuan Y-J (2013) Metabolic analysis reveals the amino acid responses of *Streptomyces lydicus* to pitching ratios during improving streptolydigin production. *Appl Microbiol Biotechnol* 97:5943–5954
- Dotzlaw JE, Metzger LS, Foglesong MA (1984) Incorporation of amino acid-derived carbon into tylactone by *Streptomyces fradiae* GS14. *Antimicrob Agents Chemother* 25:216–220
- Du W, Huang D, Xia M, Wen J, Huang M (2014) Improved FK506 production by the precursors and product-tolerant mutant of *Streptomyces tsukubaensis* based on genome shuffling and dynamic fed-batch strategies. *J Ind Microbiol Biotechnol* 41:1131–1143
- Goranovič D, Blažič M, Magdevska V, Horvat J, Kuščer E, Polak T, Santos-Aberturas J, Martínez-Castro M, Barreiro C, Mrak P (2012) FK506 biosynthesis is regulated by two positive regulatory elements in *Streptomyces tsukubaensis*. *BMC Microbiol* 12:1
- Goranovič D, Kosec G, Mrak P, Fujs Š, Horvat J, Kuščer E, Kopitar G, Petković H (2010) Origin of the allyl group in FK506 biosynthesis. *J Biol Chem* 285:14292–14300
- Höffner K, Harwood S, Barton P (2013) A reliable simulator for dynamic flux balance analysis. *Biotechnol Bioeng* 110:792–802
- Huang D, Li S, Xia M, Wen J, Jia X (2013) Genome-scale metabolic network guided engineering of *Streptomyces tsukubaensis* for FK506 production improvement. *Microb Cell Fact* 12:52
- Huang D, Wen J, Wang G, Yu G, Jia X, Chen Y (2012) In silico aided metabolic engineering of *Streptomyces roseosporus* for daptomycin yield improvement. *Appl Microbiol Biotechnol* 94:637–649
- Huang D, Xia M, Li S, Wen J, Jia X (2013) Enhancement of FK506 production by engineering secondary pathways of *Streptomyces tsukubaensis* and exogenous feeding strategies. *J Ind Microbiol Biotechnol* 40:1023–1037
- Husain S, Singh N (2002) The impact of novel immunosuppressive agents on infections in organ transplant recipients and the interactions of these agents with antimicrobials. *Clin Infect Dis* 35:53–61
- Ingram JR, Martin JA, Finlay AY (2009) Impact of topical calcineurin inhibitors on quality of life in patients with atopic dermatitis. *Am J Clin Dermatol* 10:229–237
- Jung S, Moon S, Lee K, Park Y-J, Yoon S, Yoo YJ (2009) Strain development of *Streptomyces* sp. for tacrolimus production using sequential adaptation. *J Ind Microbiol Biotechnol* 36:1467–1471

25. Kieser T, Bibb MJ, Buttner MJ, Chater KF, Hopwood DA (2000) Practical streptomyces genetics. John Innes Foundation, Norwich
26. Kim HS, Park YI (2007) Lipase activity and tacrolimus production in *Streptomyces clavuligerus* CKD 1119 mutant strains. J Microbiol Biotechnol 17:1638
27. Kino T, Hatanaka H, Hashimoto M, Nishiyama M, Goto T, Okuhara M, Kohsaka M, Aoki H, Imanaka H (1987) FK-506, a novel immunosuppressant isolated from a *Streptomyces*. I. Fermentation, isolation, and physico-chemical and biological characteristics. J Antibiot 40:1249–1255
28. Kol S, Merlo ME, Scheltema RA, de Vries M, Vonk RJ, Kikkert NA, Dijkhuizen L, Breitling R, Takano E (2010) Metabolomic characterization of the salt stress response in *Streptomyces coelicolor*. Appl Environ Microbiol 76:2574–2581
29. Laber B, Gomis-Rüth F, Romao M, Huber R (1992) *Escherichia coli* dihydrodipicolinate synthase. Identification of the active site and crystallization. Biochem J 288:691–695
30. Mahadevan R, Edwards JS, Doyle FJ (2002) Dynamic flux balance analysis of diauxic growth in *Escherichia coli*. Biophys J 83:1331–1340
31. Martínez-Castro M, Salehi-Najafabadi Z, Romero F, Pérez-Sanchiz R, Fernández-Chimeno RI, Martín JF, Barreiro C (2013) Taxonomy and chemically semi-defined media for the analysis of the tacrolimus producer '*Streptomyces tsukubaensis*'. Appl Microbiol Biotechnol 97:2139–2152
32. Meng H, Lu Z, Wang Y, Wang X, Zhang S (2011) In silico improvement of heterologous biosynthesis of erythromycin precursor 6-deoxyerythronolide B in *Escherichia coli*. Biotechnol Bioprocess Eng 16:445–456
33. Mishra A, Verma S (2012) Optimization of process parameters for tacrolimus (FK 506) production by new isolate of *Streptomyces* sp. using response surface methodology (RSM). J Biochem Technol 3:419–425
34. Mo S, Ban Y-H, Park JW, Yoo YJ, Yoon YJ (2009) Enhanced FK506 production in *Streptomyces clavuligerus* CKD1119 by engineering the supply of methylmalonyl-CoA precursor. J Ind Microbiol Biotechnol 36:1473–1482
35. Mo S, Kim DH, Lee JH, Park JW, Basnet DB, Ban YH, Yoo YJ, S-w Chen, Park SR, Choi EA (2010) Biosynthesis of the allylmalonyl-CoA extender unit for the FK506 polyketide synthase proceeds through a dedicated polyketide synthase and facilitates the mutasynthesis of analogues. J Am Chem Soc 133:976–985
36. Mo S, Lee S-K, Jin Y-Y, Oh C-H, Suh J-W (2013) Application of a combined approach involving classical random mutagenesis and metabolic engineering to enhance FK506 production in *Streptomyces* sp. RM7011. Appl Microbiol Biotechnol 97:3053–3062
37. Mo S, Lee S-K, Jin Y-Y, Suh J-W (2016) Improvement of FK506 production in the high-yielding strain *Streptomyces* sp. RM7011 by engineering the supply of allylmalonyl-CoA through a combination of genetic and chemical approach. J Microbiol Biotechnol 26:233–240
38. Mo S, Yoo YJ, Ban YH, Lee S-K, Kim E, Suh J-W, Yoon YJ (2012) Roles of fkbN in positive regulation and tcs7 in negative regulation of FK506 biosynthesis in *Streptomyces* sp. strain KCTC 11604BP. Appl Environ Microbiol 78:2249–2255
39. Nie L, Wu G, Culley DE, Scholten JC, Zhang W (2007) Integrative analysis of transcriptomic and proteomic data: challenges, solutions and applications. Crit Rev Biotechnol 27:63–75
40. Ordóñez-Robles M, Rodríguez-García A, Martín JF (2016) Target genes of the *Streptomyces tsukubaensis* FkbN regulator include most of the tacrolimus biosynthesis genes, a phosphopantetheinyl transferase and other PKS genes. Appl Microbiol Biotechnol 100:8091–8103
41. Pérez-García F, Peters-Wendisch P, Wendisch VF (2016) Engineering *Corynebacterium glutamicum* for fast production of L-lysine and L-pipecolic acid. Appl Microbiol Biotechnol 100:8075–8090
42. Pei G, Chen L, Zhang W (2017) Chapter nine-WGCNA application to proteomic and metabolomic data analysis. Methods Enzymol 585:135–158
43. Price ND, Papin JA, Schilling CH, Palsson BO (2003) Genome-scale microbial in silico models: the constraints-based approach. Trends Biotechnol 21:162–169
44. Sambrook J, Russell D (2001) Molecular cloning: a laboratory manual, 3rd edn. Cold Spring Harbor Laboratory, Cold Spring Harbor
45. Schuetz R, Zamboni N, Zampieri M, Heinemann M, Sauer U (2012) Multidimensional optimality of microbial metabolism. Science 336:601–604
46. Stuetz A, Baumann K, Grassberger M, Wolff K, Meingassner JG (2006) Discovery of topical calcineurin inhibitors and pharmacological profile of pimecrolimus. Int Arch Allergy Immunol 141:199–212
47. Su Y, Wang J, Shi M, Niu X, Yu X, Gao L, Zhang X, Chen L, Zhang W (2014) Metabolomic and network analysis of astaxanthin-producing *Haematococcus pluvialis* under various stress conditions. Biores Technol 170:522–529
48. Sui X, Niu X, Shi M, Pei G, Li J, Chen L, Wang J, Zhang W (2014) Metabolomic analysis reveals mechanism of antioxidant butylated hydroxyanisole on lipid accumulation in *Cryptocodinium cohnii*. J Agric Food Chem 62:12477–12484
49. Sun Y, Ye R (2016) Impact of a novel precursor on FK506 production and key gene transcription in *Streptomyces tsukubaensis* No. 9993. Res Chem Intermed 42:3351–3358
50. Turlo J, Gajzlerska W, Klimaszewska M, Król M, Dawidowski M, Gutkowska B (2012) Enhancement of tacrolimus productivity in *Streptomyces tsukubaensis* by the use of novel precursors for biosynthesis. Enzyme Microb Technol 51:388–395
51. Vaid S, Narula P (2006) Novel process for producing tacrolimus (FK-506) using vegetable oil as sole source of carbon. International publication patent no WO 11156:A2
52. Wang C, Liu J, Liu H, Wang J, Wen J (2017) A genome-scale dynamic flux balance analysis model of *Streptomyces tsukubaensis* NRRL18488 to predict the targets for increasing FK506 production. Biochem Eng J 123:45–56
53. Wang J, Chen L, Tian X, Gao L, Niu X, Shi M, Zhang W (2013) Global metabolomic and network analysis of *Escherichia coli* responses to exogenous biofuels. J Proteome Res 12:5302–5312
54. Wang J, Liu H, Huang D, Jin L, Wang C, Wen J (2017) Comparative proteomic and metabolomic analysis of *Streptomyces tsukubaensis* reveals the metabolic mechanism of FK506 overproduction by feeding soybean oil. Appl Microbiol Biotechnol 101:2447–2465
55. Wang J, Zhang X, Shi M, Gao L, Niu X, Te R, Chen L, Zhang W (2014) Metabolomic analysis of the salt-sensitive mutants reveals changes in amino acid and fatty acid composition important to long-term salt stress in *Synechocystis* sp. PCC 6803. Funct Integr Genom 14:431–440
56. Weatherburn M (1967) Phenol-hypochlorite reaction for determination of ammonia. Anal Chem 39:971–974
57. Wentzel A, Sletta H, Ellingsen TE, Bruheim P (2012) Intracellular metabolite pool changes in response to nutrient depletion induced metabolic switching in *Streptomyces coelicolor*. Metabolites 2:178–194
58. Werth MT, Halouska S, Shortridge MD, Zhang B, Powers R (2010) Analysis of metabolomic PCA data using tree diagrams. Anal Biochem 399:58–63
59. Wilkinson CJ, Hughes-Thomas ZA, Martin CJ, Bohm I, Mironenko T, Deacon M, Wheatcroft M, Wirtz G, Staunton J, Leadlay PF (2002) Increasing the efficiency of heterologous promoters in actinomycetes. J Mol Microbiol Biotechnol 4:417–426

60. Wu S, Hu C, Jin G, Zhao X, Zhao ZK (2010) Phosphate-limitation mediated lipid production by *Rhodospiridium toruloides*. *Biores Technol* 101:6124–6129
61. Xia M, Huang D, Li S, Wen J, Jia X, Chen Y (2013) Enhanced FK506 production in *Streptomyces tsukubaensis* by rational feeding strategies based on comparative metabolic profiling analysis. *Biotechnol Bioeng* 110:2717–2730
62. Yoon YJ, Choi CY (1997) Nutrient effects on FK-506, a new immunosuppressant, production by *Streptomyces* sp. in a defined medium. *J Ferment Bioeng* 83:599–603
63. Yu X, Niu X, Zhang X, Pei G, Liu J, Chen L, Zhang W (2015) Identification and mechanism analysis of chemical modulators enhancing astaxanthin accumulation in *Haematococcus pluvialis*. *Algal Res* 11:284–293
64. Zhang X-S, Luo H-D, Tao Y, Wang Y-Y, Jiang X-H, Jiang H, Li Y-Q (2016) FkbN and Tcs7 are pathway-specific regulators of the FK506 biosynthetic gene cluster in *Streptomyces tsukubaensis* L19. *J Ind Microbiol Biotechnol* 43:1693–1703
65. Zhao S, Huang D, Qi H, Wen J, Jia X (2013) Comparative metabolic profiling-based improvement of rapamycin production by *Streptomyces hygroscopicus*. *Appl Microbiol Biotechnol* 97:5329–5341